Jakeya Sultana, Md. Saiful Islam, Mohammad Faisal, Mohammad Rakibul Islam, Brian W.-H. Ng, Heike Ebendorff-Heidepriem, Derek Abbott

Highly birefringent elliptical core photonic crystal fiber for terahertz application

Optics Communications, 2018; 407:92-96

Published at: http://dx.doi.org/10.1016/j.optcom.2017.09.020

Highly Birefringent Elliptical Core Photonic Crystal Fiber for Terahertz Application

Jakeya Sultana[a], Md. Saiful Islam[b], Mohammad Faisal[c], Mohammad Rakibul Islam[a], Brian W.-H. Ng[b], Heike Ebendorff-Heidepriem[d], Derek Abbott[b]

[a]*Department of Electrical & Electronic Engineering, Islamic University of Technology, Gazipur 1704, Bangladesh.*
[b]*School of Electrical & Electronic Engineering, The University of Adelaide, SA 5005, Australia.*
[c]*Department of Electrical & Electronic Engineering, Bangladesh University of Engineering & Technology, Dhaka 1000, Bangladesh.*
[d]*School of Physical Sciences, The University of Adelaide, SA 5005, Australia.*

Abstract

We present a novel strategy for designing a highly birefringent photonic crystal fiber (PCF) with near zero flattened dispersion properties by applying elliptical air holes in the core area. The elliptical structure of the air holes in the porous-core region introduces asymmetry between x and y polarization modes, which consequently offers ultra-high birefringence. Also the compact geometry of the conventional hexagonal structure in the cladding confines most of the useful power. The optical properties including birefringence, dispersion, confinement loss, effective material loss (EML) and single modeness of the fiber are investigated using a full-vector finite element method. Simulation results show an ultra-high birefringence of 0.086 ultraflattened near zero dispersion of 0.53 ± 0.07 ps/THz/cm in a broad frequency range. The practical implementation of the proposed fiber is feasible using existing fabrication technology and is applicable to the areas of terahertz sensing and polarization maintaining systems.

Keywords: photonic crystal fiber, birefringence, dispersion, waveguide, effective material loss, terahertz.

Email address: `mdsaiful.islam@adelaide.edu.au` (Md. Saiful Islam)

1. Introduction

The electromagnetic frequency band lying between the technologically well-developed microwave and infrared regions is generally referred to as the terahertz band. Recently, significant attention has been given to terahertz wave propagation due to its numerous practical applications in the field of sensing [1], non-invasive medical imaging [2], spectroscopy [3], detection of defects in solar panels, characterization of dielectric materials[4], pharmaceutical drug testing, astronomy, and communication [5]. Although there has been an enormous development in terahertz wave generation and detection, most of terahertz realizations are free-space systems. Free space propagation of terahertz waves is limited by moisture in the atmosphere. So, for low loss, flexible, long distance and efficient transmission of terahertz waves, it is necessary to design guided transmission media. Keeping all of this in mind, various types of guided transmission media have been proposed in the past few years. Metallic wires [6] and metal coated dielectric tubes[7] were proposed earlier but disregarded due to their higher bending loss and lower coupling efficiency. In recent times, there has been interest in polymer fibers such as polymer Bragg fiber, polystyrene foam, plastic fiber, hollow core fiber, solid core fiber and porous core photonic crystal fiber (PCF) [8, 9, 10]. Using porous core PCF has a number of important advantages such as lower material absorption loss, lower dispersion, geometries such as pitch size, air hole radius, and core radius can be readily selected. Beside low loss, it is also necessary to design a highly birefringent fiber that has key applications in terahertz sensing, communications, and terahertz heterodyne detection. There are basically two key methods for obtaining a highly birefringent terahertz fibers, one is to break the symmetry in the cladding region and another is to introduce asymmetry in the porous core. Several types of waveguide have been proposed earlier for low loss and highly birefringent terahertz waveguide. In 2009, Atakaraminas *et al.* [11] proposed a low loss, low dispersion, and highly birefringent PCF. They introduced an asymmetrical structure in the core resulting in a birefringence of 0.026. A squeezed lattice elliptical air hole based terahertz fiber were proposed by Chen [12] *et al.* and resulted in a birefringence of the order of 10^{-2}. A dual air hole unit core based PCF has been proposed by Hasanuzzaman *et al.* [13]. They were able to obtain a moderate birefringence of 0.033 with a material absorption loss of 0.43 dB/cm. However, they neglect to report the dispersion properties of their proposed fiber. A spiral photonic crystal fiber was proposed later [14] to obtain a birefringence of 0.0483 but with a higher EML of 0.085 cm^{-1}. The dispersion variation in this case was also high. Raonaqul *et al.* [15] proposed a dual asymmetrical PCF with a birefringence of 0.045. However, their obtained EML as well as dispersion variation was much higher. An oligo-porous core [16] and triple hole core [17] fibers have also been proposed that shows a birefringence of 3×10^{-2} and 10^{-2} respectively. Recently, a birefringence value 1.19×10^{-2} with high EML of 0.0689 cm^{-1} has been exhibited by applying two layers of elliptical structure in the core [18].

In this letter, we introduce a novel Topas based photonic crystal fiber consisting of a conventional hexagonal structure in the cladding and a penta-hole elliptical structure in the core which simultaneously offering ultra-high birefringence and ultra-low near zero flattened dispersion. Several types of core structures including hexagonal [19], rhombic [20], dual hole unit [13], diamond [21], rectangular slot [22], oligo-porous [16], tri-air hole [17], hexagonal structure with elliptical shaped air holes [28] have previously been analyzed. However, to the best of our knowledge, penta-hole elliptical structure inside a hexagonal cladding has not been considered. Using the existing fabrication techniques, the proposed terahertz waveguide is feasible.

2. Design Methodology

The cross section of the proposed terahertz PCF is shown in Fig. 1. Five rings of hexagonal structure with larger air filling fraction of 0.90 are used to obtain flat dispersion properties also the penta-hole elliptical air holes in the core are use to increase birefringence. Full vector finite element based commercially available software package Comsol $v4.3b$ is used to design the proposed structure. A perfectly matched layer (PML) boundary condition with 9% radius of the

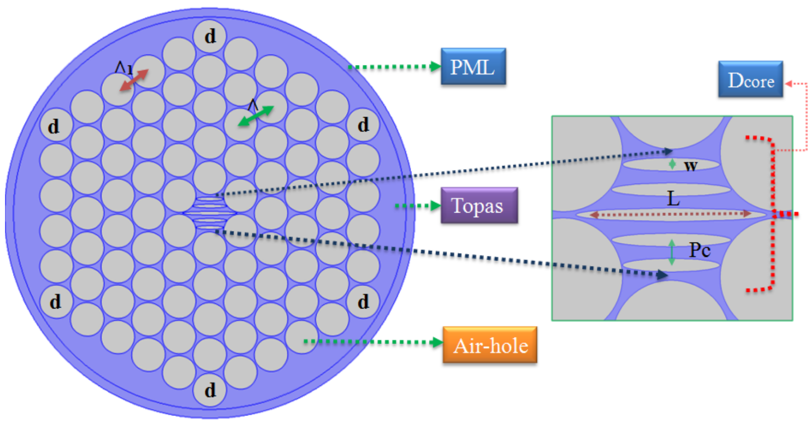

Figure 1: Schematic diagram of the proposed waveguide with its enlarged version of the core.

fiber is used at the outer part of the PCF to reduce the effect of surrounding environment. In the cladding region, the diameter of each air is set to d. The distance of air holes lies in the same ring is denoted by Λ_1 and that lies in the other rings is denoted by Λ. They are related to one another by $\Lambda_1 = 0.90\Lambda$. The core diameter is fixed to 350 μm. The diameter of the major and minor axis of the elliptical air holes has been denoted by (L) and (w) as shown in Fig. 1. For our simulation, we kept the major axis (L) fixed and varied the minor axis (w) by varying the core porosity. Furthermore, ellipticity defined as the ratio of major and minor axis of the elliptical air holes (L/w) determines the size of the elliptical air holes. Different lengths have been used to design the elliptical air holes inside the core. The center air hole has a length (L) of 255 μm; from the center air hole the length of other air holes both in upper and lower has a length of 160 μm and 130 μm respectively. The width (w) of each air hole in the core has been determined by the core porosity that can be defined as the fiber core area to the total area of the fiber. Also the core pitch P_c which can be defined as the center to center distance between two elliptical air holes has set to 6 μm. Topas has been used as the background material because of its unique characteristics including, lower bulk material absorption loss 0.2 cm^{-1}; glass transition temperature T_g much higher than PMMA; multi-antibody bio-sensing; constant refractive index $n = 1.53$ in the frequency range of 0.1–1.5 THz; and being negligibly hygroscopic [4, 23]. Throughout the whole simulation 50% porosity, 1 THz frequency and x-polarization mode is considered as optimum design parameters.

3. Simulation and Results

The mode power distribution at different core porosities for both x and y polarization is shown in Fig. 2. It is observed that, there is a large difference

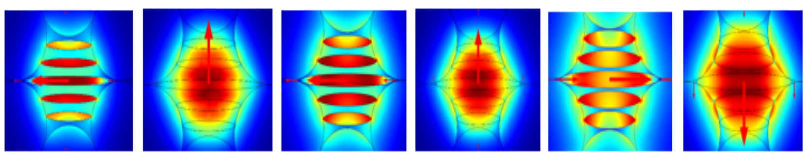

(a) (b) (c) (d) (e) (f)

Figure 2: E- field distribution for (a) 50% porosity, x-pol (b) 50% porosity, y-pol (c) 65% porosity, x-pol (d) 65% porosity, y-pol (e) 80% porosity, x-pol (f) 80% porosity, y-pol.

between the mode field distributions through the core region. As a result, there is a large effective index difference with respect to frequency between the polarization modes (Fig. 3). This is because of the large asymmetrical structure of the core air holes. The refractive index difference in the x and y polarization mode is known as birefringence. Birefringence can be calculated using the following equation [28],

$$B = |n_x - n_y| \tag{1}$$

where n_x and n_y represents the effective refractive index of x and y polarizations respectively. At different porosity values, Fig. 4 exhibit the characteristicsof birefringence variation with respect to frequency. It can be observed that, birefringence increases with the increase of frequency because such increments enhances the index contrast between the orthogonal polarization modes.

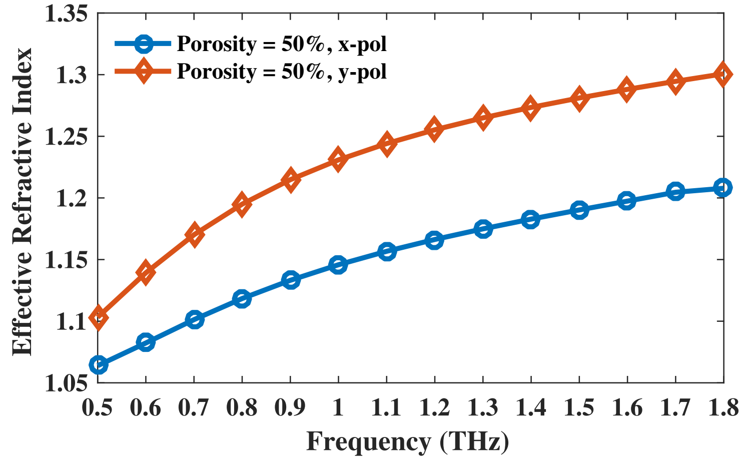

Figure 3: Effective refractive index vs frequency at optimal design parameters.

It is also observed that, at higher porosity values the amount of birefringence decreases because such increment of porosity causes some of the useful power propagates outside the core region that reduces the index contrast between the polarization modes which consequently reduces the birefringence. At optimal design parameters, the obtained birefringence is 0.086, which is better than the previously proposed [11, 12, 13, 14, 15, 16, 17, 18, 28] terahertz waveguides.

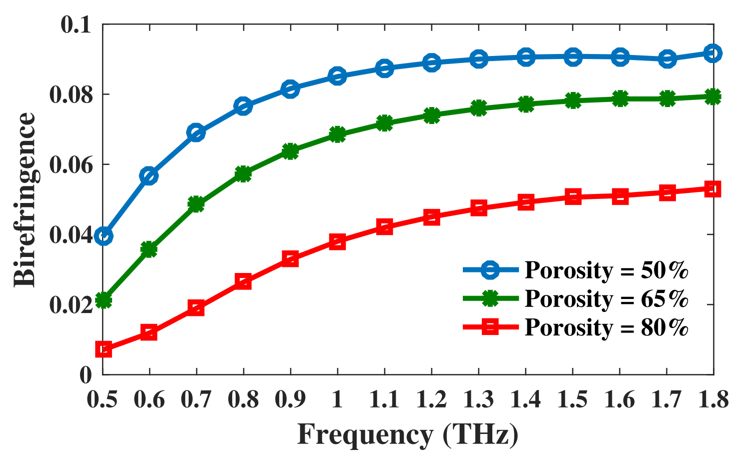

Figure 4: Birefringence vs frequency at different porosities with 350 μm core diameter.

The main difficulty of designing a terahertz waveguide is its high EML. So, for efficient transmission of terahertz waves it is necessary to design a low loss waveguide. The material absorption loss or EML of a fiber can be calculated by [27],

$$\alpha_{\text{eff}} = \sqrt{\frac{\epsilon_0}{\mu_0}} \left(\frac{\int_{\text{mat}} n_{\text{mat}} |E|^2 \alpha_{\text{mat}} dA}{|\int_{\text{all}} S_z dA|} \right). \tag{2}$$

Here, n_{mat} is the effective refractive index of Topas COC, α_{mat} is the bulk material absorption loss of Topas, ϵ_0 and μ_0 is the relative permittivity and permeability of free space, S_z is the z-component of the Poynting vector $S_z = \frac{1}{2}(E \times H^*)z$. where E and H^* are the electric and magnetic field components. The effective material loss as a function of frequency is shown in Fig. 5. It can be observed that, as the frequency increases the EML also increases linearly which meets the theoretical consequences of calculating EML according to the empirical formula $\alpha(\nu) = \nu^2 + 0.63\nu - 0.13$ [dB/cm], [27]. It is also observed that, EML increases with the decrease of porosity because reducing porosity means reducing the core air hole diameter which in turn increase the amount of material inside the core area. At optimal design parameters, a very small amount of EML of 0.05 cm^{-1} is obtained which is comparable with the previously reported [11, 12, 13, 14, 15, 16, 17, 18] fibers.

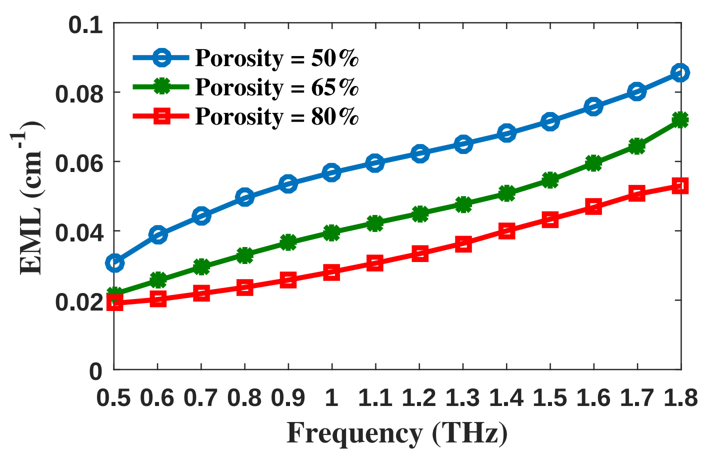

Figure 5: EML vs frequency at different porosities and 350 μm core diameter.

Confinement loss is another loss mechanism which limits the length of terahertz signal transmission. This confinement loss occurs due to the finite number of air hole rings in the cladding that can be calculated by the following equation [26],

$$L_c = 8.686 \left(\frac{2\pi f}{c}\right) \mathrm{Im}(n_{\mathrm{eff}}), \mathrm{dB/cm}. \tag{3}$$

Here, $\mathrm{Im}(n_{\mathrm{eff}})$ represents the imaginary part of the complex refractive index, f is the operating frequency and c is the speed of light. It is seen in Fig. 6 that, con-

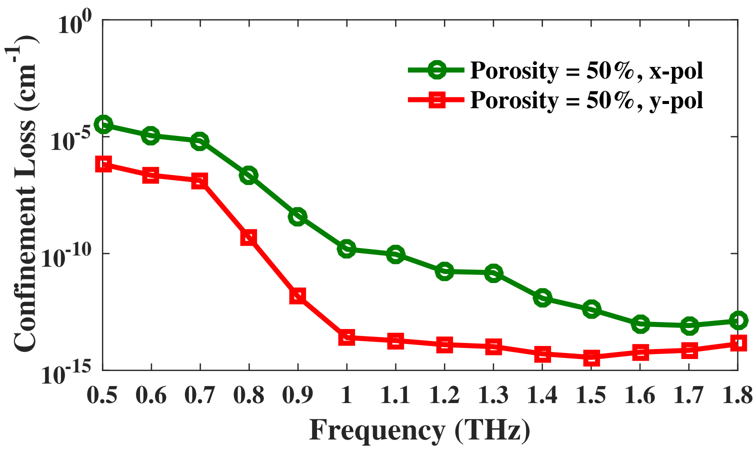

Figure 6: Confinement loss vs frequency at optimal design parameters.

finement loss rapidly drops with increase in frequency because the mode power begins to constrict strictly in the porous core region [27]. It is found that, a very low confinement loss of the order of 10^{-9} cm^{-1} is obtained at optimal design parameters. It can be mentioned that; the obtained value of confinement loss is negligible compared to the obtained EML.

Low and flat dispersion is impressive for applications in the terahertz frequency range. Dispersion properties of a fiber can be calculated by [28],

$$\beta_2 = \frac{2}{c}\frac{dn_{\mathrm{eff}}}{dw} + \frac{w}{c}\frac{d^2 n_{\mathrm{eff}}}{dw^2}, \mathrm{ps/THz/cm}. \tag{4}$$

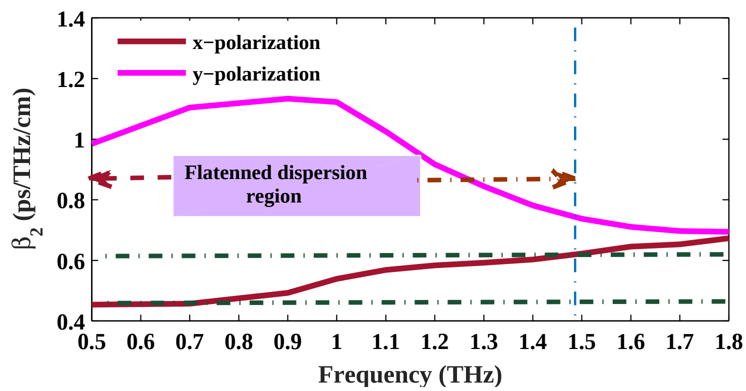

Figure 7: Dispersion vs frequency for both x and y polarization mode.

Where, c is the speed of light, n_{eff} is the effective refractive index of the core, ω is the angular frequency. Fig. 7 indicates the dispersion variation with respect to frequency. It can be seen that, at optimal design parameters the obtained dispersion is 0.53 ± 0.07 ps/THz/cm within a broad frequency range of 0.5–1.48 THz. The obtained dispersion is very low and flat also significantly improved over previously reported optical waveguide designs [11, 12, 13, 14, 15, 16, 17, 18], [24, 25, 26, 27, 28].

Long-distance transmission of signals with nearly zero interference requires the use of single-mode PCF. The single mode condition of a fiber can be calculated using equation [29],

$$V = \frac{2\pi f}{c}\sqrt{n_{\text{co}}^2 - n_{\text{cl}}^2} \leq 2.405. \tag{5}$$

Here, n_{co} and n_{cl} represents the effective refractive index of the core and cladding respectively. From the waveguide design, it can be observed that, the cladding mainly consists of a large number of air holes, thus most of the previously reported [24, 14] waveguides considered that value as unity, but practically the value should be greater than unity [27] because the cladding not only consists of air holes but also consists of bulk material. The value of n_{co} is equal to the effective refractive index of the core. In Eqn. 5 it is clearly stated that, to operate a fiber into single mode region the value of V-parameter must not exceed 2.405.

So, observing Fig. 8 it can be said that, our proposed waveguide operates in the single mode condition.

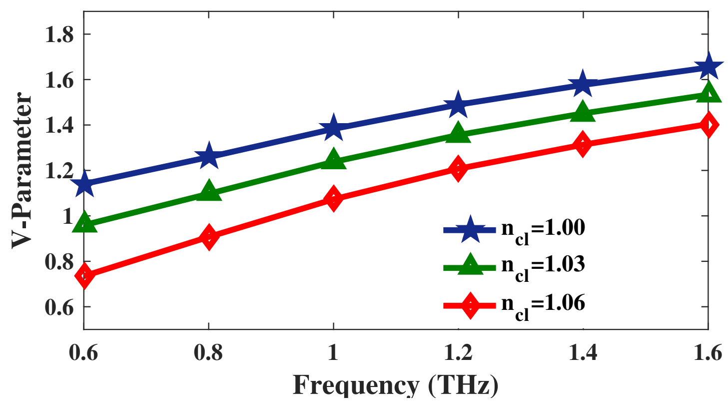

Figure 8: V-parameter vs frequency at optimal design parameters.

For practical implementation of our proposed waveguide, it is necessary to address the fabrication possibilities thoroughly. There are several fabrication techniques developed in recent years. Among them, capillary stacking, stack and drilling, sol-gel techniques are only capable of fabricating circular shaped air holes. To fabricate asymmetrical structures Atakaramians *et al.* [11], [28] experimentally employed an extrusion technique [29]. Issa et. al [33] fabricated elliptical air holes in 2004. Moreover, the previously published articles [34] [35] [36] reported that the elliptical air hole patterns can be fabricated using the existing fabrication technology. In addition, Liu et al. [37] used the methyl methacrylate (MMA) monomer polymerization method to fabricate elliptical air holes. Moreover, jiang et al.[30] recently used 3D printed dies and got improvement of fiber drawing over "stack and draw"and extruded preforms. They used the 3D printed technique to fabricate not only elliptical air holes but also other complex structures. Moreover, Microstructured optical fibers (MOFs) with different sizes of core and cladding air holes has already been fabricated using the extrusion technique [38], [39]. As our proposed waveguide consists of conventional hexagonal structure in the cladding and elliptical structure in the core, it is amenable to existing fabrication techniques.

In Table 1 the characteristics comparison of our proposed PCF with some other terahertz waveguide. It is clearly seen that, the proposed PCF shows excellent characteristics for polarization maintaining terahertz application in addition for flattened dispersion application. Using the elliptical air hole structure in the core, the obtained birefringenc is highest than ever proposed by any terahertz waveguide.

Table 1: Comparison of characteristics of the proposed PCF with other PCF's

Ref.	f (THz)	Por(%)	B	β_2(ps/THz/cm)	α_{eff}	L_c
[13]	0.85	-	0.033	-	0.43 dB/cm	$10^{-3.8}$ cm^{-1}
[14]	1	-	0.0483	0.51	0.085 cm^{-1}	0.00191 dB/cm
[15]	1	-	0.045	0.26	0.08 cm^{-1}	-
[16]	3	30	0.03	$0.2-1$	0.06 cm^{-1}	0.01 dB/m
[17]	3	60	0.01	$0-1.5$	0.04 cm^{-1}	0.01 dB/m
[18]	1	55	0.0119	-	0.0689 dB/cm	-
[31]	1	84	-	0.09	0.034 cm^{-1}	$10^{-3.7}$ cm^{-1}
[32]	1	83	-	0.05	0.03 cm^{-1}	$10^{6.5}$ cm^{-1}
This manuscript	1	50	0.086	0.07	0.05 cm^{-1}	10^{9} cm^{-1}

4. Conclusion

A novel photonic crystal fiber with ultra-high birefringence and near zero flattened dispersion has been proposed. Numerical results indicate a very high birefringence of 0.086 and near zero flat dispersion 0.53±0.07 ps/THz/cm can be obtained within a broad frequency range of 0.5–1.48 THz. In addition, the proposed waveguide exhibits a negligible confinement loss of 10^{-9} cm^{-1} at 1 THz frequency. Potential applications are anticipated in the areas of sensing, terahertz communication systems and polarization preserving fibers.

References

[1] D. Abbott and X. C. Zhang, "T-ray imaging, sensing, and retection," *Proceedings of the IEEE.*, vol. 95, no. 8, pp. 1509–1513, 2007.

[2] W. Withayachumnankul, G. M. Png, X. Yin, S. Atakaramians, I. Jones, H. Lin, B. S. Y. Ung, J. Balakrishnan, B. W. H. Ng, B. Ferguson, S. P. Mickan, B. M. Fischer, and D. Abbott, "T-ray sensing and imaging," *Proceedings of the IEEE.*, vol. 95, no. 8, pp. 1528–1558, 2007.

[3] W. Withayachumnankul, *Engineering aspects of terahertz time-domain spectroscopy,* Ph.D thesis, (The University of Adelaide, 2009).

[4] J. Balakrishnan, B. M. Fischer, and D. Abbott, "Sensing the hygroscopicity of polymer and copolymer materials using terahertz time-domain spectroscopy," *Appl. Opt.*, vol 48, no. 12, pp. 2262–2266, 2009.

[5] M. Nagel, P. H. Bolivar, M. Brucherseifer, H. Kurz, A. Bosserhoff and R. Bttner, "Integrated THz technology for label-free genetic diagnostics," *Applied Physics Letters.*, vol 80, pp. 154–156, 2002.

[6] K. Wang and D. M. Mittleman, "Metal wires for terahertz waveguiding," *Nature.*, vol. 432, pp. 376–379, 2004.

[7] B. Bowden, J. A. Harrington, and O. Mitrofanov, "Silver/polystyrenecoated hollow glass waveguides for the transmission of terahertz radiation," *Opt. Lett.*, vol. 32, no 20, pp. 2945–2947, 2007.

[8] J. Y. Lu, C. P. Yu, H. C. Chang "Terahertz air-core microstructure fiber," *Opt. Lett.*, vol. 92, no 6, 064105, 2007.

[9] M. Skorobogatiy, and A. upuis, "Ferroelectric all-polymer hollow Bragg fibers for terahertz guidance," *Appl. Phys. Lett.*, vol. 90, no. 11, 113514, 2007.

[10] G. Zhao, M. T. Mors, T. Wenckebach,"Terahertz dielectric properties of polystyrene foam," *J. Opt. Soc. Am. B,*, vol. 19, no. 6, pp.1476–1479, 2007.

[11] S. Atakaramians, S. Afshar V, B. M. Fischer, D. Abbott, and T. M. Monro, "Low loss, low dispersion and highly birefringent terahertz porous fibers," *Opt. Commun.*, vol. 282, no. 1, pp. 36−38, 2009.

[12] H. B. Chen, D. R. Chen, and Z. Hong, "Squeezed lattice elliptical hole terahertz fiber with high birefringence," *Appl. Opt.*, vol. 48, no. 20, pp. 3943−3947, 2009.

[13] G. K. M. Hasanuzzaman, Sohel Rana and M. S. Habib, "A novel low loss, highly birefringent photonic crystal fiber in THz regime," *IEEE Photon. Technol. Lett.*, vol. 28, no. 8, pp. 899−902, 2016.

[14] M. R. Hasan, M. S. Anower, M. A. Islam, and S. M. A. Razzak, "Polarization-maintaining low-loss porous-core spiral photonic crystal fiber for terahertz wave guidance," *Appl. Opt*, vol. 55, no. 15, pp. 4145−4152, 2016.

[15] R. Islam, M. S. Habib, G. K. M. Hasanuzzaman, S. Rana and A. Sadat, "Novel porous fiber based on dual-asymmetry for low-loss polarization maintaining THz wave guidance," *Opt. Express*, vol. 41, no. 3, pp. 440−443, 2016.

[16] Z. Wu, Z. Shi, H. Xia, X. Zhou, Q. Deng, J. Huang, X. Jiang, and W. Wu "Design of highly birefringent and low-loss oligoporous-core THz Photonic crystal fiber with single circular air-hole unit," *IEEE Photonics Journal*, vol. 8, no. 6, 4502711, 2016.

[17] Z. Wu, X. Zhou, H. Xia, Z. Shi, J. Huang, X. Jiang, and W. Wu, "Low-loss polarization-maintaining THz photonic crystal fiber with a triple-hole core," *Appl. Opt.*, vol. 56, no. 8, pp. 2288−2293, 2017.

[18] K. Ahmed, S. Chowdhury, B. K. Paul, M. S. Islam, S. Sen, M. I. Islam, and S. Asaduzzaman "Ultrahigh birefringence, ultralow material loss porous core single-mode fiber for terahertz wave guidance," *Appl. Opt.*, vol. 56, no. 12, pp. 3477–3483, 2017.

[19] R. Islam, G. K. M. Hasanuzzaman, Md. S. Habib, S. Rana, and M. A. G. Khan, "Low-loss rotated porous core hexagonal single-mode fiber in THz regime," *Opt. Fiber Technol.*, vol. 24, pp. 38–43, 2015.

[20] Md. Rabiul Hasan, Md. Ariful Islam, M. S. Anower, and S. M. A. Razzak "Low-loss and bend-insensitive terahertz fiber using a rhombic-shaped core," *Appl. Opt.*, vol. 55, no. 30, pp. 8441–8447, 2016.

[21] Sohel Rana, Md. Saiful Islam, Jakeya Sultana, Mohammad Rakibul Islam, Mohammad Faisal, Samaun Reza, Ashfaq Ahmed "A highly birefringent slotted-core THz fiber," *International Conference on Electrical and Computer Engineering,*, 2016. DOI: 10.1109/ICECE.2016.7853897.

[22] C. Markos, A. Stefani, K. Nielsen, H. K. Rasmussen, W. Yuan, O. Bang, "High-Tg TOPAS microstructured polymer optical fiber for fiber Bragg grating strain sensing at 110 degrees," *Opt. Express.*, vol 21, no. 4, pp. 4758–4785, 2013.

[23] M. S. Islam, S. Rana, M. R. Islam, M. Faisal, H. Rahman, and J. Sultana, "Porous core photonic crystal fiber for ultra-low material loss in THz regime," *IET Communications*, vol. 10, no. 16, pp. 2179–2183, 2016.

[24] S. Islam, M. R. Islam, M. Faisal, A. S. M. S. Arefin, H. Rahman, J. Sultana, and S. Rana, "Extremely low-loss, dispersion flattened porous-core photonic crystal fiber for terahertz regime," *Optical Engineering.*, vol. 55, no. 7, pp. 076117, 2016.

[25] M. S. Islam, J. Sultana, S. Rana, M. R. Islam, M. Faisal, S. F. Kaijage, and D. Abbott "Extremely low material loss and dispersion flattened TOPAS based circular porous fiber for long distance terahertz wave transmission," *Optical Fiber Technol.*, vol. 24, pp. 6–11, 2016.

[26] M. S. Islam, J. Sultana, J. Atai, D. Abbott, S. Rana, and M. R. Islam, "Ultra low loss hybrid core porous fiber for broadband applications," *Applied Optics.*, vol. 56, no. 9, pp. 1232–1237, 2017.

[27] S. Rana, M. S. Islam, M. Faisal, K. C. Roy, R. Islam, and S. F. Kaijage, "Single-mode porous fiber for low-loss polarization maintaining terahertz transmission," *Opt. Eng.*, vol. 55, no. 7, pp. 076114, 2016.

[28] S. Atakaramians, S. Afshar, H. Ebendorff-Heidepriem, M. Nagel, B. M. Fischer, D. Abbott, and T. M. Monro, "THz porous fibers: design, fabrication and experimental characterization," *Opt. Express.*, vol 17, no. 16, pp. 14053–14062, 2009.

[29] H. Ebendorff-Heidepriem and T. M. Monro, "Extrusion of complex preforms for microstructured optical fibers," *Opt. Express.*, vol 15, no. 23, pp. 15086−15092, 2007.

[30] X. Jiang, N. Y. Joly, R. Sopalla, F. Babic, J. Huang, and P. Russell, "Soft Glass Microstructured Fibers and Their Applications,," *in Advanced Photonics 2016 (IPR, NOMA, Sensors, Networks, SPPCom, SOF), OSA Technical Digest (online) (Optical Society of America*, paper SoW3G.1.(2016).

[31] J. Sultana, Md. S. Islam, J. Atai, M. R. Islam and D. Abbott "Near-zero dispersion flattened, low-loss porous-core waveguide design for terahertz signal transmission," *Opt. Eng.*, vol. 56, no. 7, 076114 (2017).

[32] Md. S. Islam, J. Sultana, J. Atai, M. R. Islam and D. Abbott, "Design and Characterization of a Low-Loss, Dispersion-Flattened Photonic Crystal Fiber for Terahertz Wave Propagation," *Optik - International Journal for Light and Electron Optics.*, vol. 145, 398–406 (2017).

[33] N. A. Issa, M. A. V. Eijkelenborg, M. Fellew, F. Cox, G. Henry, and M. C. J. Large, "Fabrication and study of microstructured optical fibers with elliptical holes," *Opt. Lett.*, vol 29, no. 12, pp. 1336–1338, (2004).

[34] S. Asaduzzaman, K. Ahmed, T. Bhuiyan, and T. Farah, "Hybrid photonic crystal fiber in chemical sensing," *SpringerPlus*, vol 5, no. 748, pp. 1–11, (2016).

[35] S. Asaduzzaman and K. Ahmed, "Proposal of a gas sensor with high sensitivity, birefringence and nonlinearity for air pollution monitoring," *Sens. Bio-Sens. Res.* , vol 10, pp. 20–26, (2016).

[36] S. Asaduzzaman, K. Ahmed, M. F. H. Arif, and M. Morshed, "Application of microarray-core based modified photonic crystal fiber in chemical sensing," *1st International Conference on Electrical & Electronic Engineering (ICEEE)* , pp. 41–44, (2015).

[37] F. Liu, H. Gao, Q. Xu, and Y. Zhang, "Fabrication and Characteristics of Elliptical-Holes and near Elliptical Core Hexangular Lattice Photonic Crystal Fibers Based on Polymer," *Advanced Materials Research*, vol. 279, pp. 151–156, (2011).

[38] Y. Ruan, H. Ebendorff-Heidepriem, S. Afshar, and T. M. Monro, "Light confinement within nanoholes in nanostructured optical fibers," *Opt. Express*, vol. 18, no. 25, pp. 26018–26026, (2010).

[39] W. Q. Zhang, H. Ebendorff-Heidepriem, T. M. Monro, and S. Afshar , "Fabrication and supercontinuum generation in dispersion flattened bismuth microstructured optical fiber," *Opt. Express*, vol. 19, no. 22, pp. 21135–21144, (2011).